Journal of Seismic Response Control Systems, Vol. 1, pp. 1 – 24, 2025
https://doi.org/10.65423/0p52sc25

Effectiveness of Particle Tuned Mass Dampers in Buildings Subjected to Narrow-Band Seismic Excitations

Miguel A. Jaimes
Institute of Engineering, UNAM, Mexico City, Coordinación de Ingeniería Estructural.
mjaimest@iingen.unam.mx

Francisco A. Godínez
Institute of Engineering, UNAM, Mexico City; Unidad de Investigación y Tecnología Aplicadas, UNAM, Apodaca Nuevo Leon.
fgodinezr@iingen.unam.mx

Received: 9 April 2025. **Accepted**: 4 August 2025. **Published**: 26 November 2025

Abstract

This study evaluates the effectiveness of Particle Tuned Mass Dampers (PTMD) in attenuating structural vibrations in buildings subjected to narrow-band seismic excitations. PTMDs are passive energy dissipation devices capable of reducing the lateral response of the primary structural system. First, the maximum displacement response of a single-degree-of-freedom (SDOF) system was assessed for three configurations: 1) a SDOF system without a damper; 2) a SDOF system with a Tuned Mass Damper (TMD); and 3) a SDOF system with a PTMD. Then, the response of 11-storey and 17-storey three-bay reinforced concrete linear frames with PTMDs, TMDs, and without dampers was analyzed under narrow-band seismic motions. Results indicate that the main advantage of a PTMD is the significant reduction in lateral displacements and accelerations when the ratio between the predominant frequencies of the ground motion and the building is close to unity, and the first mode dominates the structural response. The findings of this study provide guidance for practicing engineers to assess the feasibility of using PTMDs in new or existing structures subjected to narrow-band earthquake excitations, in regions such as Mexico City.

Keywords: Particle tuned mass dampers (PTMDs), narrow-band seismic excitations, displacement demand, floor acceleration, Mexico City earthquakes.

1. Introduction

Civil structures, such as tall buildings, can be susceptible to seismic and wind loads. Under these excitations, excessive displacements and accelerations can occur at the top of buildings, causing discomfort to users. In other circumstances, when excitations are sufficiently intense, structural damage, even catastrophes, can occur [1]. For these reasons, it is essential to take actions for controlling excessive vibrations to prevent disasters. One means of achieving this is by employing a mechanical device composed of an elastic element, a damping element and a moving mass known as a tuned mass damper (TMD). This concept was first introduced by Frahm in 1911 [2] to reduce the rolling motion of ships as well as hull vibrations. Later, Ormondroyd and Den Hartog proposed a theory of TMD [3], followed by a detailed analysis of the optimum tuning and damping parameters in Den Hartog's book on mechanical vibrations [4]. The TMD technology has been traditionally used to passively suppress and control vibrations in structures [5-13].

However, the frequency spectrum with which the TMD can work properly is limited. Another option with wider suppression frequency bands is the particle damper (PD). The applications of these devices cover many and varied fields since this technology demands low manufacturing costs, can be adapted to almost any geometry and it is not strongly affected by environmental conditions, particularly temperature, which can have adverse effects on the performance of viscoelastic materials that are often used for isolation and vibration damping [14-24]. PDs, however, are not very sensitive to frequency as TMDs are [25]. Thus arose the concept of the particle tuned mass damper (PTMD), which combines valuable characteristics of both particle dampers and tuned mass dampers [25-26]. Accordingly, PTMDs are passive control systems that dissipate the input energy by tuning the frequency as in the case of TMDs, and by collisions among particles, impacts between particles and container walls, friction and sound radiation as occurs in PDs. Up to now, however, research on the effectiveness of PTMDs in controlling the structural response due to earthquakes is still at an early stage of theoretical and experimental development [27-32].

Consequently, only few examples of practical application can be found [33-34], and in contrast, a considerable amount of basic research focused on structural vibration attenuation has been published. Lu et al. [35] performed an experimental parametric study to evaluate the performance of a one-story steel frame equipped with a PTMD; and in this way, they also developed a simplified numerical method to optimally design the particle damper. Similarly, to this research, there are many papers where the coupled response of elastic systems with PTMDs is the central research objective [26, 32, 35-36]. The results of these investigations show that, in general, the PTDMs installed on elastic systems are effective in reducing the maximum story displacement; furthermore, the internal forces on a frame with PTMDs can be significantly lower than those without dampers of this type. The performance of both TMDs and PTMDs is highly dependent on their tuning. Optimally tuned devices can significantly enhance vibration mitigation by properly matching their dynamic properties—such as mass, stiffness, and damping—with those of the primary structure. In particular, achieving the appropriate frequency and damping ratios is critical for maximizing energy dissipation during seismic events. As a result, selecting adequate tuning parameters becomes a fundamental step in the design process of these devices. In this context, the main objective of

the present study is to evaluate the effectiveness of PTDMs in attenuating vibrations in buildings located in highly seismic regions such as Mexico City.

The proposed analysis takes into consideration buildings with very common structural characteristics (particularly 11- and 17-storey structures) in this city; and subjected to highly destructive seismic events such as the infamous 1985 and 2017 earthquakes. To our knowledge there are very few, if any, studies that address these peculiarities, despite being very necessary to develop protective measures and standards to better address the damage and destruction associated with high intensity telluric events. A secondary objective is to give more diffusion to the concept of PTMD particularly among the civil engineering community in Mexico, because according to what has been investigated and presented in this introduction, PTDMs are not yet popular despite their higher performance compared to traditional TMD systems. The earthquake-induced response of single-story buildings with PTMDs is first studied to find appropriate PTMD parameters for controlling lateral displacements. For this matter, the governing differential equations of SDOF systems with PTMDs and TMDs (and without them for comparison purposes) under transient excitations are solved. Three types of arrangements are examined: 1) a SDOF system without dampers; 2) a SDOF system with TMDs and 3) a SDOF system with PTMDs.

Then, the responses of 11- and 17-storey three-bay reinforced concrete linear frames with PTMDs and tuned mass dampers (TMDs), and without them, are analyzed considering the suitable parameters found for the three SDOF systems listed above. These two building configurations were selected because their fundamental periods (approximately 1.4 s and 2.0 s) are representative of structures in Mexico City that are prone to resonance under narrow-band seismic excitations, making them ideal case studies for assessing PTMD effectiveness. The study considers narrow-band ground motions recorded at two sites located at Mexico City, which are known to generate a significant amount of energy content within a narrow range of structural periods [37]. When structural systems are subjected to narrow-band ground motions with long duration, their capacity to dissipate energy is decreased as the structural period tends to zero. The amount of energy input to the structural systems due to narrow-band ground motions is substantial, as compared to the energy introduced by wide-band ground motions [37]. Therefore, this study allows assessing the effectiveness of PTMDs in buildings for reducing the lateral response subjected to narrow-band seismic excitations.

Results of the structural response analysis for buildings in Mexico City under seismic events, as those well-known destructive earthquakes of 1985 and 2017, allow the formulation of guidelines for the applicability of PTMDs and the proper design parameters of these attenuation devices at such powerful seismic environments.

2. Procedure description

The effectiveness of structures with PTMDs under narrow-band seismic excitations is described in two parts: (i) assessment of the earthquake-induced dynamic response on SDOF systems with PTMDs and TMDs and without them; and (ii) determination of the lateral response of 11- and 17-storey frames with the passive control devices and without them. These two stages are detailed below.

2.1 Analysis of SDOF systems

The response of a SDOF system is studied herein for three configurations: (1) a SDOF system without dampers; (2) a SDOF system with a TMD; and (3) a SDOF system with a PTMD (Fig. 1). In this study, a TMD is a passive control device added to the top portion of the system, which consist of a mass suspended on pendulum rods, tuned to certain natural frequency of the system. In this way, certain significant kinetic energy is transferred from the main structure to the suspended mass and dissipated by the TMD ([38], Fig. 1b). On the other hand, a PTMD is a container suspended on pendulum rods attached to the top of the system, and inside it there are one or more particles, which through collisions between them, collisions between particles and the walls of the container, friction and sound radiation can suppress the vibrations of the main system (Fig. 1c). Ground motions are input as horizontal base accelerations.

2.1.1 SDOF structure without dampers

The equation of motion of a SDOF structure, as shown in Fig. 1a, is presented. The governing second order differential equation is given by:

$$\ddot{u}_1 = -\ddot{u}_g - 2\xi_1\omega_1\dot{u}_1 - \omega_1^2 u_1 \tag{1}$$

In Eq. (1), $\ddot{u}_1$ denotes the SDOF's acceleration, $\ddot{u}_g$ denotes the input ground acceleration, $\omega_1 = \sqrt{k_1/m_1}$ is the undamped frequency (where m_1 is the mass and k_1 is the stiffness), and $\xi_1 = c_1/2m_1\omega_1$ is the nominal viscous damping ratio of the SDOF oscillator i.e., primary structural system.

2.1.2 SDOF structure with tuned mass damper

The seismic response of a SDOF structure with a TMD, as depicted in Figure 1b, can be computed with the formulation presented by [39]:

$$\ddot{u}_1 = -\ddot{u}_g - 2\xi_1\omega_1\dot{u}_1 + \gamma 2\xi_2\omega_2(\dot{u}_2 - \dot{u}_1) - \omega_1^2 u_1 + \gamma\omega_2^2(u_2 - u_1) \tag{2}$$

$$\ddot{u}_2 = -2\xi_2\omega_2(\dot{u}_2 - \dot{u}_1) - \omega_2^2(u_2 - u_1) \tag{3}$$

In the system of Eqs. (2) and (3), $\ddot{u}_2$ represents the TMD system's acceleration, $\omega_2 = \sqrt{k_2/m_2}$ is the undamped frequency (where m_2 is the mass and k_2 is the stiffness of the TMD system), and $\xi_2 = c_2/2m_2\omega_2$ is the nominal viscous damping ratio of the TMD system. On the other hand, in Eq. (2), $\gamma = m_2/m_1$ is the mass ratio between the TMD system and SDOF oscillator.

Notice that when the parameter γ is equal to zero into Eq. (2), the formulation proposed in the literature for the case of the elastic SDOF oscillator is obtained. Similarly, when the parameter $m_2 = 0$ also $\ddot{u}_2 = 0$ and therefore the Eq. (3) is missing.

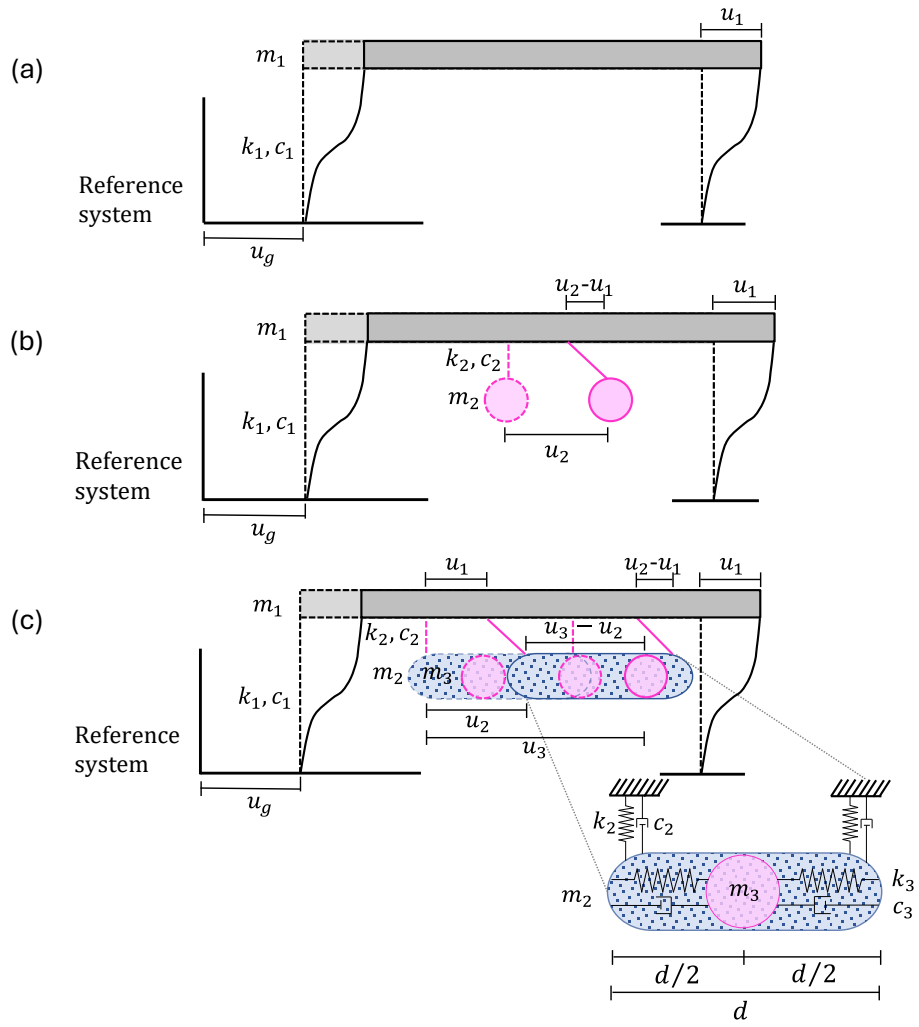

Fig 1. Schematic view of SDOF systems: a) without dampers; b) with a TMD and c) with a PTMD.

2.1.3 SDOF structure with particle tuned mass damper

Analogous to Eqs. (2) and (3), the equations of motion for SDOF structures with PTMDs (Fig. 1c), were formulated in [11] and [36]. The governing set of equations is

$$\ddot{u}_1 = -\ddot{u}_g - 2\xi_1\omega_1\dot{u}_1 + \gamma 2\xi_2\omega_2(\dot{u}_2 - \dot{u}_1) - \omega_1^2 u_1 + \gamma\omega_2^2(u_2 - u_1) \tag{4}$$

$$\ddot{u}_2 = -2\xi_2\omega_2(\dot{u}_2 - \dot{u}_1) + \beta 2\xi_3\omega_3 H(\delta, \dot{\delta}) - \omega_2^2(u_2 - u_1) + \beta\omega_3^2 G(\delta) \tag{5}$$

$$\ddot{u}_3 = -2\xi_3\omega_3 H(\delta, \dot{\delta}) - \omega_3^2 G(\delta) \tag{6}$$

In Eq. (4), $\ddot{u}_3$ represents the acceleration of the particle; $\omega_3 = \sqrt{k_3/m_3}$ are the undamped frequency (where m_3 is the mass of the particle and k_3 is the stiffness of interaction between the particle and the container), and $\xi_3 = c_3/2m_3\omega_3$ is the idealized viscous damping ratio between the particle and the container. In Eq. (5), $\beta = m_3/m_2$ is the mass ratio between the particle and the container. Finally, in Eqs. (5) and (6), $G(\delta)$

and $H(\delta, \dot{\delta})$ describe the relative displacement $\delta = u_3 - u_2$ and velocity $\dot{\delta} = \dot{u}_3 - \dot{u}_2$, of the particle with respect to the container during the impact process, which are associated with the nonlinear stiffness and damping of the impact damper ([11,14], Figure 2). When $\beta = 0$ in Eq. (5) the model given by [39] is recovered.

According to Figure 2, the PTMD dissipates energy by collision between the particle and the container walls only when $|\delta| - d/2 \geq 0$ (d is the gap clearance between the particle and the container i.e., the length of the container). As long as no collision occurs between the particle and the container wall (i.e., $|\delta| - d/2 < 0$), the PTMD works as a TMD, i.e., the vibration of the primary structural system is attenuated solely through momentum transfer.

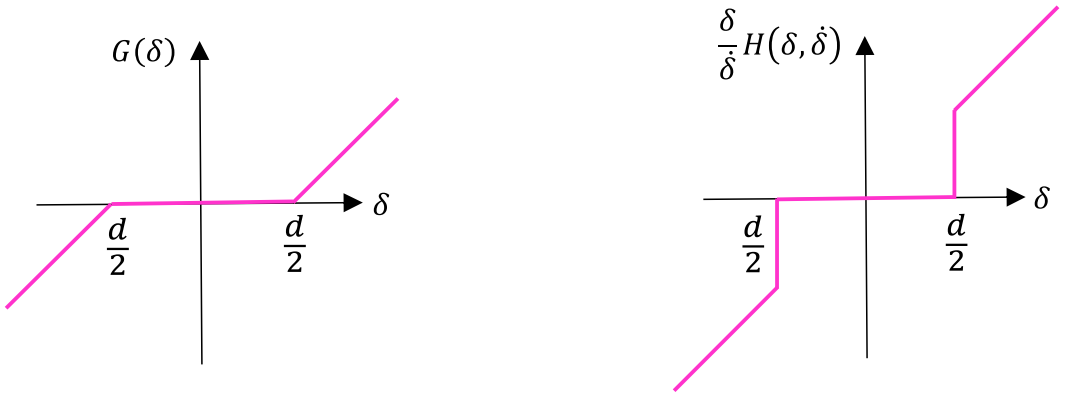

Fig 2. Nonlinear functions characterizing $G(\delta)$ (left) and $H(\delta, \dot{\delta})$ (right) between the particle and the container [11, 14].

2.1.4 Solving scheme for differential equations

The solution of Eqs. (1) to (6) were obtained through a numerical scheme based on the explicit (fourth order) Runge-Kutta method [40]. A time integration step (Δt) equal to 10^{-4} s was used for the integration of the entire recording of each narrow-band ground motion.

2.2 Analysis of 11- and 17-storey elastic frames

The frames analyzed in this study are representative of buildings with fundamental periods of 1.4 and 2 s, respectively, having a plant of 12×12 m^2. The height of all stories is 3 m high (see Figure 3). These structural periods fall within the range where resonance phenomena are typically observed in soft-soil sites like Mexico City during narrow-band seismic events. Thus, these configurations not only reflect realistic urban typologies but also enable a meaningful comparison between simplified SDOF models and more complex MDOF responses when equipped with PTMD or TMD systems. The cross-sections of the girders vary from 0.2×0.4 m at the lower levels, to 0.3×0.5 m at the top stories. The dimensions of the columns vary from 0.5×0.5 m at the first stories, to 0.4×0.4 m at the top levels. These dimensions and material properties, including the modulus of elasticity, were selected to ensure that the structural periods of the frames matched the target values of 1.4 s and 2.0 s. A damping ratio of 5% of critical was assumed for the structural

frames, which corresponds to commonly accepted values in seismic analysis of elastic reinforced concrete buildings. This value is used to represent the inherent energy dissipation typically observed in mid- and high-rise structures under moderate to strong shaking. A total weight W_t of 9,456 and 24,590 kN was obtained for the 11- and 17-storey elastic frames, respectively.

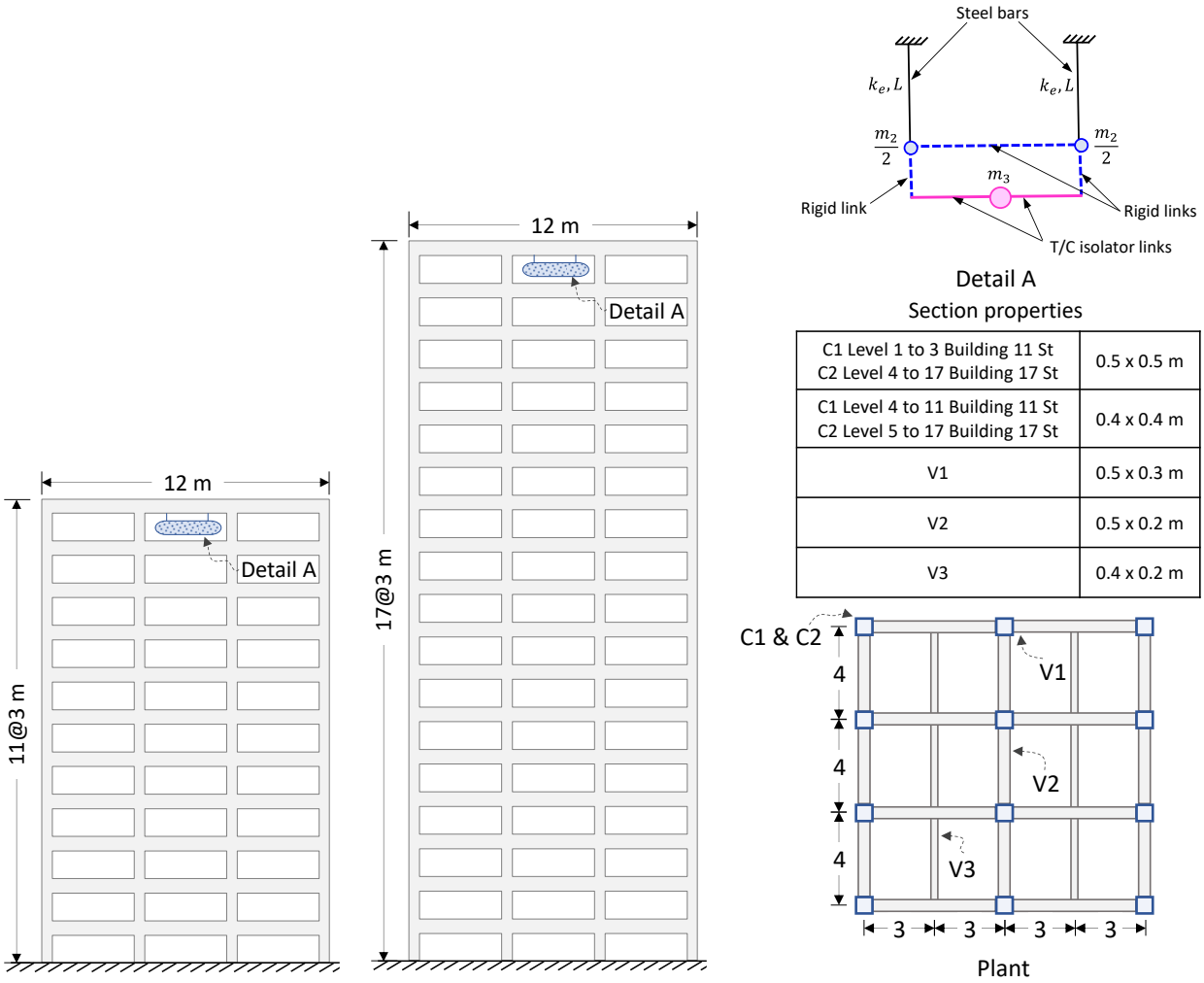

Section properties

C1 Level 1 to 3 Building 11 St C2 Level 4 to 17 Building 17 St	0.5 x 0.5 m
C1 Level 4 to 11 Building 11 St C2 Level 5 to 17 Building 17 St	0.4 x 0.4 m
V1	0.5 x 0.3 m
V2	0.5 x 0.2 m
V3	0.4 x 0.2 m

Fig 3. Geometries and properties of buildings under study.

The response of the frames without a damper was compared with that of similar systems with TMDs and PTMDs at their tops. The TMD and PTMD devices were represented by an equivalent SDOF system suspended on the top of the primary structure by two steel bars with the same length L, as shown in Fig. 3, top right corner. The length of each steel bar is considered equivalent to that of a single pendulum computed as:

$$L = g\left(\frac{T_2}{2\pi}\right)^2 \tag{7}$$

In Eq. (7), $T_2 = 2\pi/\omega_2$ is the natural period of the TMD device or the container of the PTMD device and g is the acceleration due to gravity. As will be shown in sections 3.2 and 3.3, using period ratios between the container and the frame T_2/T_1 of 0.6 and 0.7, values of $T_2 = 1.4 \times 0.6 = 0.84$ s and $T_2 = 2 \times 0.7 = 1.4$ s are computed, for the 11- and 17-storey elastic frames, respectively. Therefore, values of L equal to 0.175 and 0.487 m are obtained for such frames.

The equivalent lateral stiffness k_2 given by the two steel bars, which consider the interaction between the TMD system or the container of the PTMD device and the primary structural system, is computed as

$$k_2 = 2k_e \tag{8}$$

In Eq. (8), $k_e = 3EI/L^3$, E and I are the lateral stiffness, the modulus of elasticity and inertial moment, respectively, of each bar suspended on the top of the primary structure.

The upper ends of the steel bars are fixed in the primary structure; while their lower ends are joined to the container box by rigid joints so that they remain rigidly connected during the analysis; the mass of the container m_2 is proportionally concentrated at the ends (detail A in Fig. 3). Finally, in the case of PTMD device, to model the interaction between the particle and the container walls, tension/compression (T/C) isolator links between the particle and the container walls were used (detail A in Fig. 3, [41]), which allow free separation when the particle moves within the distance $d/2$ (i.e., the half of the gap clearance between the particle and the container), but come into contact when the particle collides with the container wall (i.e., $|\delta| - d/2 \geq 0$). These T/C isolator links are capable to simulate the impact transmission due to collision between the mass of particle m_3 and the container wall with a certain stiffness k_3 and damping constant $c_3 = 2m_3\,\xi_3\omega_3$ according to the required characteristics of interaction between the particle and the container given by Eqs. (5) and (6). This allows to model the dissipation of energy due to impact forces between the particle and the container walls. In this study, a small damping ratio $\xi_3 = 0.004$ was used for the particle, following previous works (e.g., Lu et al., 2012), in which the particle is assumed to move nearly freely inside the container until impact. This value captures the low internal damping during free motion and allows energy dissipation to be realistically concentrated during collisions.

3. Study cases

First, the earthquake-induced response of single-story buildings equipped with PTMDs is studied to determine suitable parameter values for these damping devices to control lateral displacements under narrow-band seismic excitations. Then, the response of 11- and 17-storey three-bay reinforced concrete linear frames with PTMDs and TMDs and without them are analyzed considering such suitable parameters. Finally, conclusions are given based on the results.

3.1 Strong ground motions

The earthquake-induced response of SDOF structures with TMDs and PTMDS during narrow-band ground motions is highly sensitive to spectral acceleration, duration, and frequency content, as well as other intensity measures. The influence of the frequency content of the ground motion on the SDOF structure

response is accounted for in this study by using two different narrow-band seismic records, representative of high-intensity motions obtained at CH84 and SCT stations, which are installed over soft soil sites. Both stations are situated on clay soils, known as the lakebed zone in Mexico City. These stations are of particular importance since they recorded the most intense and destructive seismic motions in Mexico City. The first one corresponds to a seismic event of $M_w = 7.1$, occurred in September 19, 2017 (CH84-17). The second one corresponds to the seismic event occurred in September 19, 1985 (SCT-85), with magnitude $M_w = 8.1$. Figure 4 displays the SA acceleration (left) and SD displacement (right) response spectra of the records used in this study. These depictions show that the soil dominant period, T_s, is about 1.4 and 2 s for sites CH84 and SCT, respectively. This means that frequency ratios between the predominant frequency of the ground earthquake excitation and the predominant frequency of each building under study is close to unity.

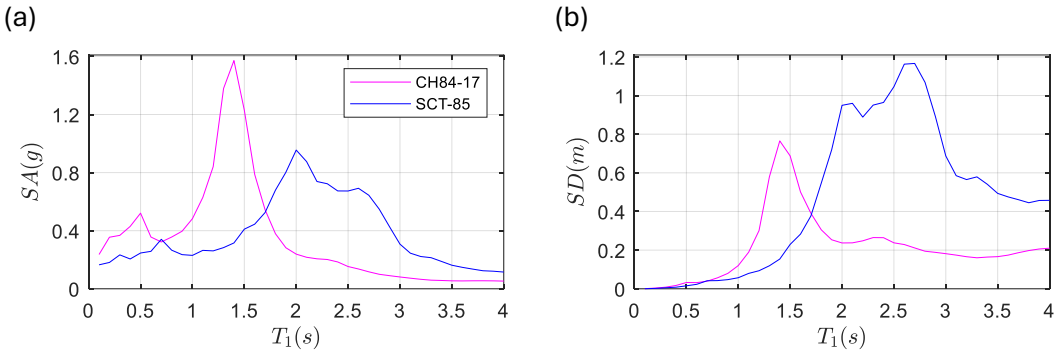

Fig 4. Acceleration (SA, left) and displacement (SD, right) response spectra of input ground motions in Mexico City.

3.2 Earthquake-Induced Dynamic Response OF SDOF structures

The earthquake-induced response of SDOF structures with PTMDs during narrow-band ground motions, which could improve the performance of new structures or existing structures in Mexico City (see Figure 1), is exemplified. For all SDOF systems, the periods of T_1 were considered equal to 1.4 and 2 s, for CH84 and SCT sites, respectively. The damping ratio ξ_1 was assumed equal to 5% of critical.

3.2.1 Parameters Influencing PTMD's Response

The response of the systems without dampers were compared with that of similar systems with added TMDs and PTMDs at their tops. The influence of the following four system parameters on the vibration control effects is investigated: (1) the period ratio between the PTMD container and SDOF oscillator, T_2/T_1; (2) the period ratio between the particle and the container T_3/T_2; (3) the mass ratio between the container and SDOF oscillator m_2/m_1; and (4) the mass ratio between the particle and the container m_3/m_2. Figures 5(a)-5(d) show the effect of these ratios (T_2/T_1, T_3/T_2, m_2/m_1, m_3/m_2) on the maximum displacement u_1 of the SDOF systems with PTMDs (solid lines) subjected to the motions CH84-17 (left, system with $T_1 = T_s = 1.4\ s$) and SCT-85 (right, system with $T_1 = T_s = 2\ s$) considering a range of gap clearance between the particle and the container $0.1 \leq d \leq 1\ m$ i.e., the length of the container. The dashed and dash-dotted lines in each plot in Fig. 5 are the response of SDOF systems and SDOF systems with TMDs, respectively.

From Figs. 5a-5d, the following observations are made:

1. The influence of the period ratio T_2/T_1 is significant in the PTMD's response. As shown in Fig. 5a, when the period ratio T_2/T_1 is less than 1 and d values are small, the system with PTMDs achieves smaller displacements with respect to those with TMDs or simply SDOF. For instance, for period ratio values T_2/T_1 of approximately 0.6 (left, system $T_1 = 1.4\ s$ subjected to motion CH84-17) and 0.7 (right, system $T_1 = 2\ s$) subjected to motion SCT-85), the lowest values of maximum displacements u_1 are reached. However, it is important to note a special case (left panel, system with $T_1 = 1.4\ s$ subjected to CH84-17 ground motion) in which the use of a PTMD can still be recommended when $T_2/T_1 \approx 1$ and d is large, as this combination results in minimal displacements. Additionally, notice that an increase in period ratio T_2/T_1 (i.e., $T_2/T_1 > 1.5$) leads to increasing displacements, reaching a TMD's behavior.

2. The period ratio T_3/T_2 is another important parameter. In Fig. 5b can be appreciated that as the period ratio T_3/T_2 increases ($T_3/T_2 > 1$), the maximum displacements also increase for the system subjected to CH84-17 (Fig. 5b left) and SCT-85 (Fig. 5b right) motions. On the contrary, when the period ratio T_3/T_2 is less than 1, as well as for small d values, the system with PTMDs achieves smaller displacements with respect to those with TMDs or simply SDOF systems.

3. The mass ratio m_2/m_1 is another key factor. In Fig. 5c can be seen that for mass ratio values m_2/m_1 larger than 0.1 and small d values, smaller displacements can be achieved with respect to those with TMDs or simply SDOF systems.

4. Finally, the mass ratio m_3/m_2 is a key factor as well. Analogous to Fig. 5c, in Fig. 5d can be seen that for mass ratio values m_3/m_2 larger than 1 and small d values, smaller displacements can be achieved with respect to those with TMDs or simply SDOF oscillators.

5. Appendix A shows plots of the maximum container displacements u_2 versus each of the four parameters analyzed in Fig. 5. The curves in this appendix show comparable trends to those in Fig. 5.

The configurations that achieved the lowest peak displacements in the SDOF simulations were selected as the basis for the PTMD and TMD properties implemented in the MDOF building models. Although no formal optimization algorithm was used, this parametric approach ensured that the adopted values were among the most effective combinations for the selected seismic inputs.

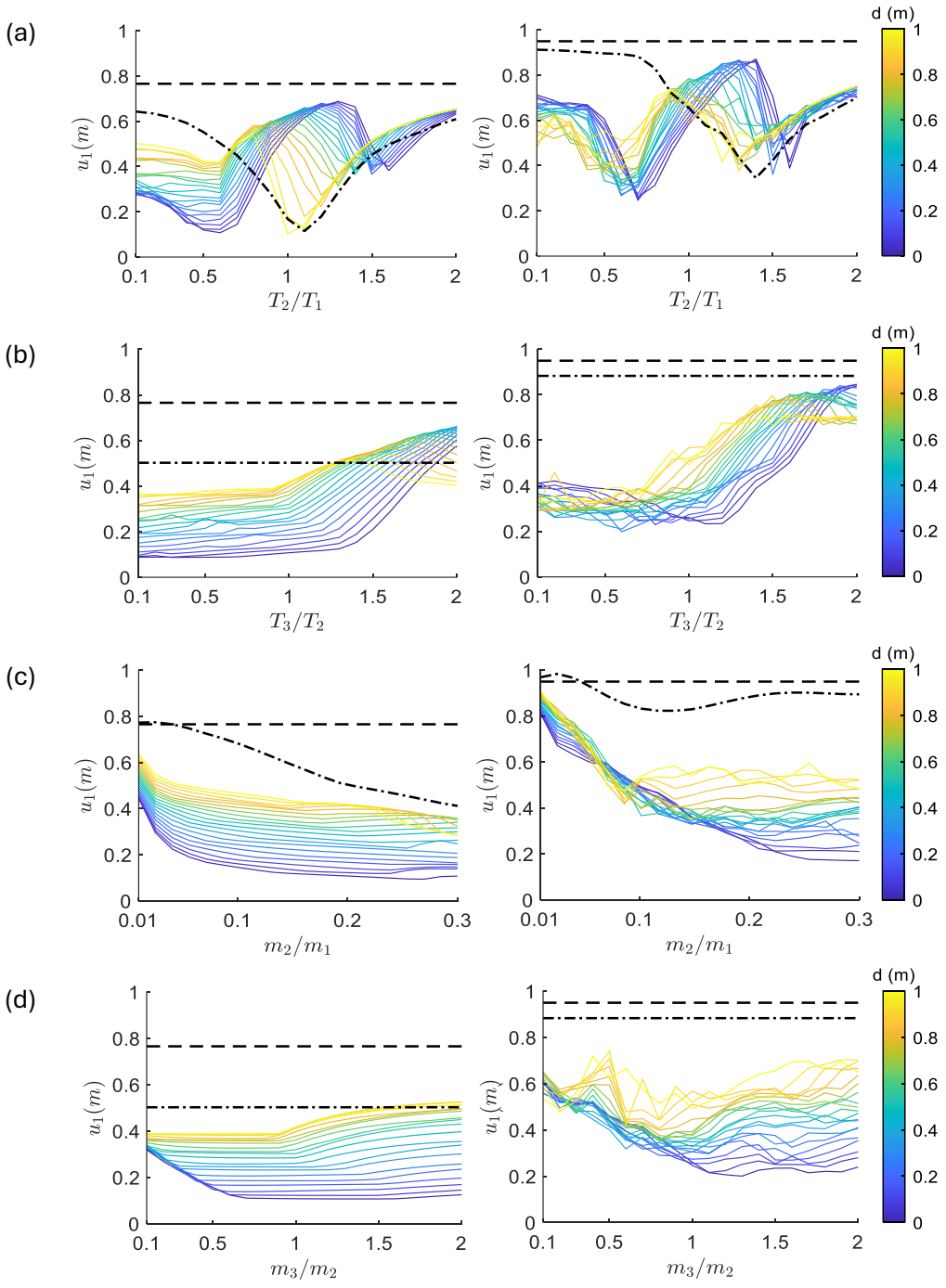

Fig 5. Contours of maximum displacements u_1 (in meters) for SDOF systems without dampers (dashed line), with TMD (dash-dotted line) and with PTMD (solid lines) subjected to the motions CH84-17 (left, $T_1 = 1.4\ s$) and SCT-85 (right, $T_1 = 2\ s$) considering the effects of: (a) the period ratio between the container and the SDOF oscillator T_2/T_1 with $\gamma = m_2/m_1 = 0.2$; $\beta = m_3/m_2 = 1$; (b) the period ratio between the particle and the container T_3/T_2 with $\gamma = m_2/m_1 = 0.2$; $\beta = m_3/m_2 = 1$; (c) the mass ratio between the container and SDOF oscillator m_2/m_1 with $\beta = m_3/m_2 = 1$; and (d) the mass ratio between the particle and the container m_3/m_2, $\gamma = m_2/m_1 = 1$. For cases (b)-(d), values of $T_2 = 0.6T_1 = 0.6\ s$ and $T_2 = 0.7T_1 = 0.7\ s$ as well as $\xi_1 = \xi_2 = 0.05$ and $\xi_3 = 0.004$ for the system subjected to CH84-17 and SCT-85 motions were considered, respectively.

3.2.2 Displacement time histories of the primary structural system

The displacement history-time response of SDOF systems subjected to the ground motion recorded at CH84 ($PGA = 0.23g$; Figure 6a, left) and SCT ($PGA = 0.16g$; Figure 6b, right) stations from the September 19th, 2017, M_w 7.1 intermediate depth instraslab and September 19th, 1985, M_w 8.1 subduction interface earthquakes, respectively, are shown in Figure 6 (input ground motions are shown in the 1st row from top). The frequency content of these narrow-band ground motions plays a key role in the displacement demand. For example, it is observed that displacements are larger for the SCT site (i.e., low frequency ground motion around 0.52 Hz, right) than those for the CH84 site (i.e., high frequency ground motions around 0.76 Hz, left). Also, this figure shows how the participation of the TMDs (3rd row from top) but mainly the PTMDs (4th row from top) could have an important effect in inducing smaller maximum displacements in the structure compared with the SDOF system without dampers (2nd row from top). Additionally, a direct comparison of the response of SDOF with TMDs and PTMDs is shown with the response of the SDOF system without dampers (gray lines). Results illustrate that displacement for SDOF system decrease significantly if the SDOF system is couple with TMDs (3rd row from top) and PTMDs (4th row from top).

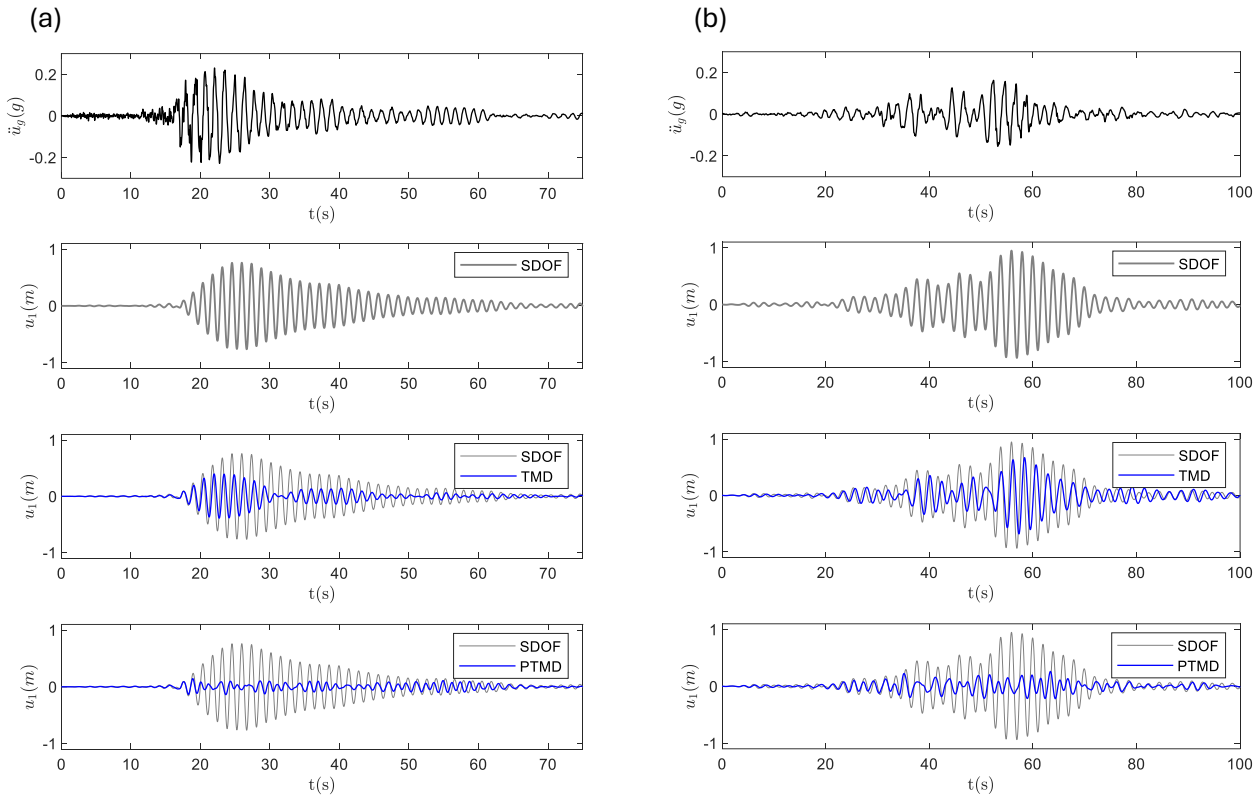

Fig 6. Displacement history-time response of SDOF systems subjected to the September 19th 2017 and September 19th 1985 earthquakes recorded at stations (left) CH84 with $PGA = 0.23g$, $T_1 = 1.4$ s, $T_2 = 0.6T_1$, $T_3 = T_2$, $\gamma = 0.2$, $\beta = 1$, $d = 0.2\ m$; and (right) SCT with $PGA = 0.16g$, , $T_1 = 2$s, $T_2 = 0.7T_1$, $T_3 = T_2$, $\gamma = 0.2$, $\beta = 1$, $d = 0.2\ m$. 1st row from top: input ground motion; 2nd row from top: SDOF without dampers; 3rd row: SDOF with TMD and 4th row: SDOF with PTMD.

3.2.3 Acceleration time histories of the primary structural system

Analogously to Figure 6, the acceleration history-time response of SDOF systems subjected to the ground motion recorded at CH84-17 and SCT-85 stations, are shown in Figure 7 (input ground motions are shown in the 1st row from top). The participation of the TMDs (3rd row from top) but mainly the PTMDs (4th row from top) have an important effect in reducing vibration effects, inducing smaller floor accelerations in the structure compared with the SDOF system without dampers (2nd row from top). Also, a direct comparison of the response of SDOF system with TMDs and PTMDs is shown together with the response of the SDOF without dampers (gray lines). Results illustrate that acceleration for SDOF system decreases significantly if the SDOF system is coupled with TMDs (3rd row from top) and PTMDs (4th row from top).

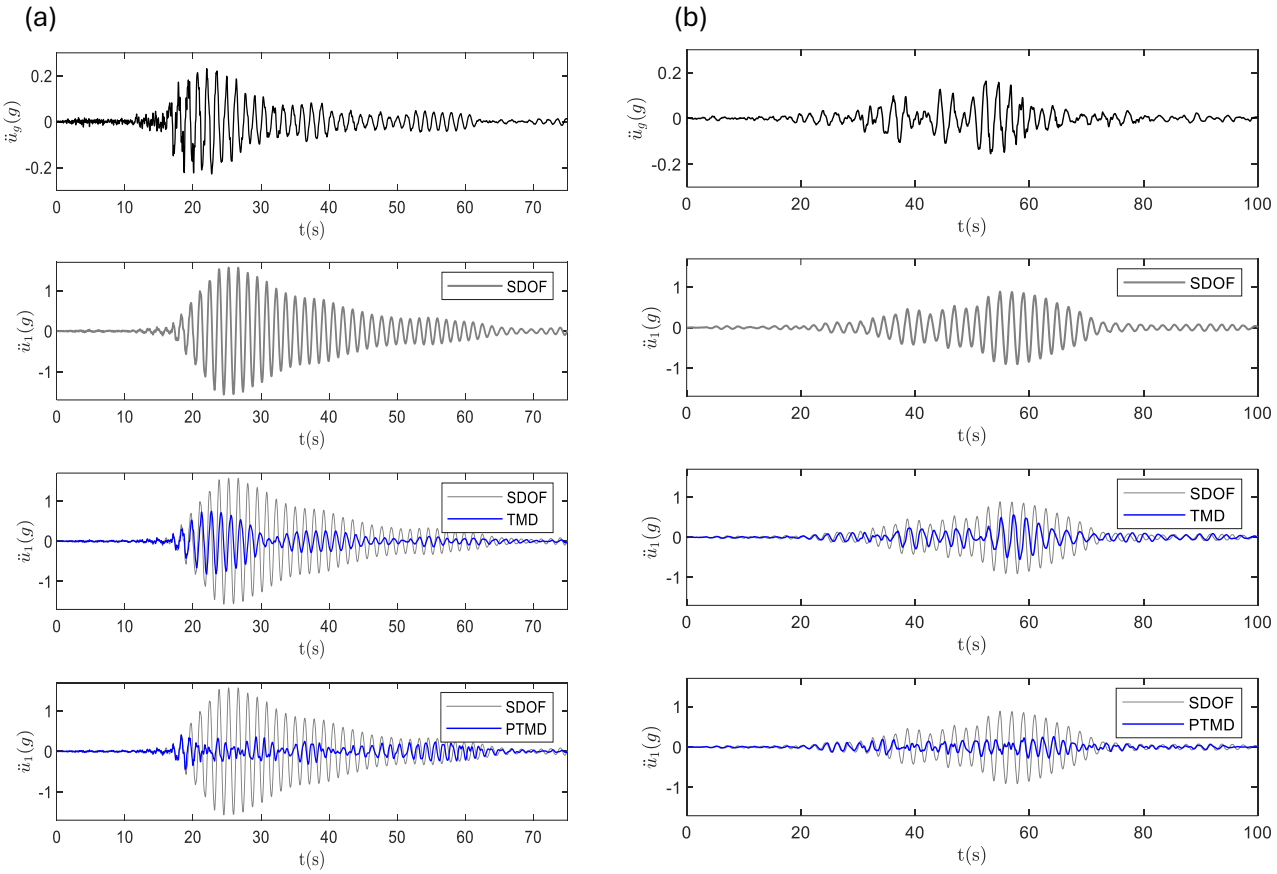

Fig 7. Acceleration history-time response of SDOF systems subjected to the September 19th 2017 and September 19th 1985 earthquakes recorded at stations (left) CH84 with $PGA = 0.23g, T_1 = 1.4s, T_2 = 0.6T_1, T_3 = T_2, \gamma = 0.2, \beta = 1, d = 0.2\ m$; and (right) SCT with $PGA = 0.16g, T_1 = 2s, T_2 = 0.7T_1, T_3 = T_2, \gamma = 0.2, \beta = 1, d = 0.2\ m$. 1st row from top: input ground motion; 2nd row from top: SDOF without dampers; 3rd row: SDOF with TMD and 4th row: SDOF with PTMD.

3.2.4 Response spectra of a SDOF system with PTMD

To depict the influence of the frequency content of the narrow-band ground motions at the seismic response of a SDOF system with PTMD, the study uses a set of synthetic ground motions computed in

accordance with 2023 Mexico City Seismic Design Provisions [42] for each study site. The seed ground motions were obtained from CH84 and SCT stations recorded on September 19th, 2017 and September 19th, 1985, respectively. These design ground motions preserve the main characteristics of the seed records; for instance, the frequency content and intensities take into account the variation of soil dominant period, T_S, due to the drying process that occurs in the lacustrine zone of the city. In Figure 8 the SA acceleration (up) and SD displacement (bottom) seismic response of a SDOF system with PTMD as described by Eqs. (4) to (6) (blue lines) is compared with the response of the same simple SDOF system computed by Eq. (1) (pink lines) subject to the synthetic ground motions for CH84 (Fig. 8a) and SCT (Fig. 8b) sites. The first observation in Fig. 8 is that, for both study sites, the SDOF system with PTMD (blue lines) is effective in reducing peak accelerations and displacements when the ratio between predominant frequencies of the ground earthquake excitation and the main system are close to unity i.e., $T_1/T_s \sim 1$. The second observation in Fig. 8 is that this situation reverts to frequency ratios far from unity e.g., $T_1/T_s > 1$, at which time the SDOF system with PTMD can result in larger displacements and accelerations.

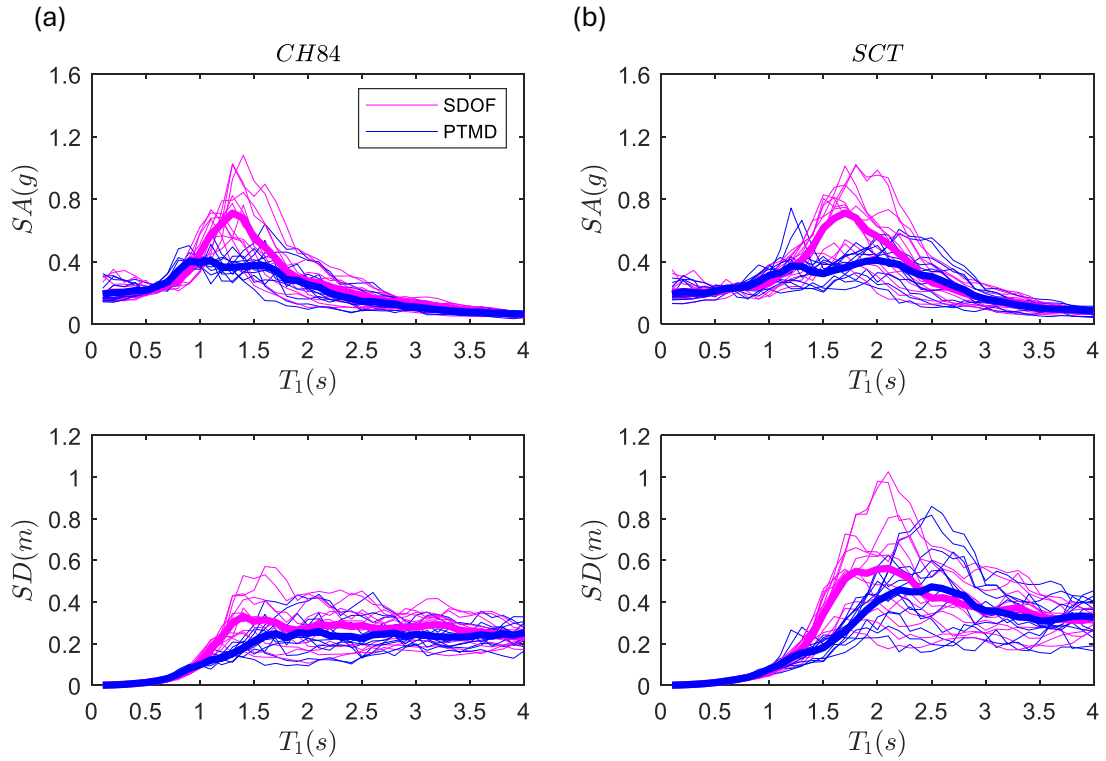

Fig 8. Response spectra of a simple SDOF system (pink lines) and a SDOF system with PTMD (blue lines) subjected to a set of design accelerograms associated to a return period of 250 years: (a) CH84 with $T_2 = 0.6T_1$, and (b) SCT with $T_2 = 0.7T_1$ For all cases, values of $T_3 = T_2, \gamma = 0.2, \beta = 1, d = 0.2\ m, \xi_1 = \xi_2 = 0.05$ and $\xi_3 = 0.004$ were considered.

3.3 Earthquake-Induced Dynamic Response of11- AND 17-storey elastic frames

The earthquake-induced response of multiple-story buildings (MDOF) with PTMDs during narrow-band ground motions, which could improve the performance of new structures or existing structures in Mexico

City (see Figure 3), is illustrated. In this study, 11- and 17-storey elastic frames with periods T_1 of 1.4 and 2 s, for CH84 and SCT sites, are considered respectively. The damping ratio ξ_1 was assumed equal to 5% of critical. More details are presented in Section 2.2.

3.3.1 Displacement time histories of the primary structural system

The response at the top of the 11-storey elastic frame when subjected to the ground motion recorded at CH84 station ($PGA = 0.23g$; left) and the response at the top of the 17-storey elastic frame when subjected to the ground motion recorded at SCT station ($PGA = 0.16g$; right) corresponding to the September 19th, 2017 and September 19th, 1985 earthquakes, respectively, are shown in Figure 9 (input ground motions are shown in the 1st row from top). The properties of the TMDs and PTMDs were defined in terms of their mass ratios with respect to that of the main frame ($\gamma = 0.2$ for both frames), their damping values ($\xi_1 = \xi_2 = 0.05$ and $\xi_3 = 0.004$), by the ratios of their natural periods to that of the frame ($T_2 = 0.6T_1 = 0.84s$ and $T_2 = 0.7T_1 = 1.4$ s for 11- and 17-storey elastic frames, respectively), by the ratios of their particle periods to that of the container ($T_3 = T_2 = 0.84\ s$ and $T_3 = T_2 = 1.4\ s$ for 11- and 17-storey elastic frames, respectively) and by the gap clearance between the particle and the container ($d = 0.2m$). As described in the previous section, the TMDs and PTMDs and parameters used were found to be adequate to control lateral displacements of SDOF systems. Therefore, the response of elastic frames is compared with the response of such SDOF systems (dashed lines). Results of displacement time histories at the top of the primary structural system (i.e., 11- and 17-storey elastic frames, solid lines) are consistent with that computed with the responses of SDOF systems (dashed lines). This verifies that the model used to represent the PTMD device successfully matched results by Eq. (3). This also shows that the use of PTMD devices effectively reduce the lateral response of the primary structural system when subjected to narrow-band seismic excitations, mainly when frequency ratios between the predominant frequency of the ground earthquake excitation and the predominant frequency of the building is close to unity and the first mode of the frame becomes dominant.

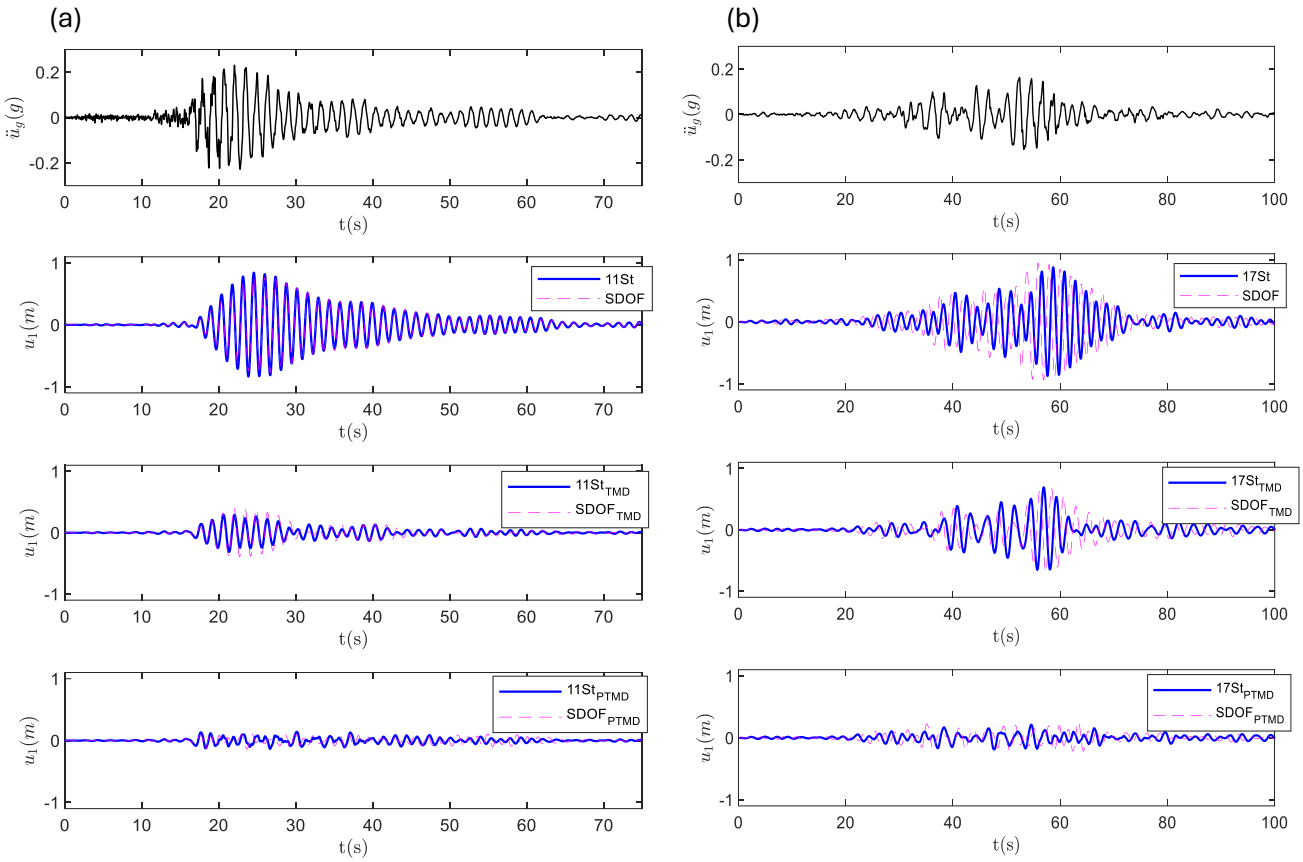

Fig 9. Displacement history-time response of 11- and 17-storey systems at the top subjected to the September 19th 2017 (left) and September 19th 1985 (right) earthquakes, respectively, recorded at CH84 station with $PGA = 0.23g, T_1 = 1.4\ s, T_2 = 0.6T_1, T_3 = T_2, \gamma = 0.2, \beta = 1, d = 0.2\ m$; and SCT station with $PGA = 0.16g, T_1 = 2\ s, T_2 = 0.7T_1, T_3 = T_2, \gamma = 0.2, \beta = 1, d = 0.2\ m$. 1st row from top: input ground motion; 2nd row from top: frame without dampers; 3rd row: frame with TMD and 4th row: frame with PTMD. The solid and dashed lines in each plot are the response of MDOF and SDOF systems, respectively.

3.3.2 Acceleration time histories of the primary structural system

Similarly, to Fig. 9, the acceleration time-history response at the 11- and 17-storey elastic frames subjected to the ground motion CH84-17 (Figure 10a, left) and SCT-95 (Figure 10b, right), are shown in Figure 10 (input ground motions are shown in the 1st row from top). The properties of the TMDs and PTMDs were defined previously. Additionally, the response of elastic frames is compared with the response of SDOF systems (dashed lines). Evidently, acceleration time histories at the top of the primary structural system (i.e., 11- and 17-storey elastic frames) are in good agreement with those computed for SDOF systems. Again, this validates the model (Eqs. (4) to (6)) used to represent the PTMD. Also, it is clear that the use of PTMD devices could reduce the floor acceleration of the primary structural system when subjected to narrow-band seismic excitations, mainly when frequency ratios between the predominant frequency of the ground earthquake ex-citation and the predominant frequency of the building is close to unity and the first mode of the frame becomes dominant.

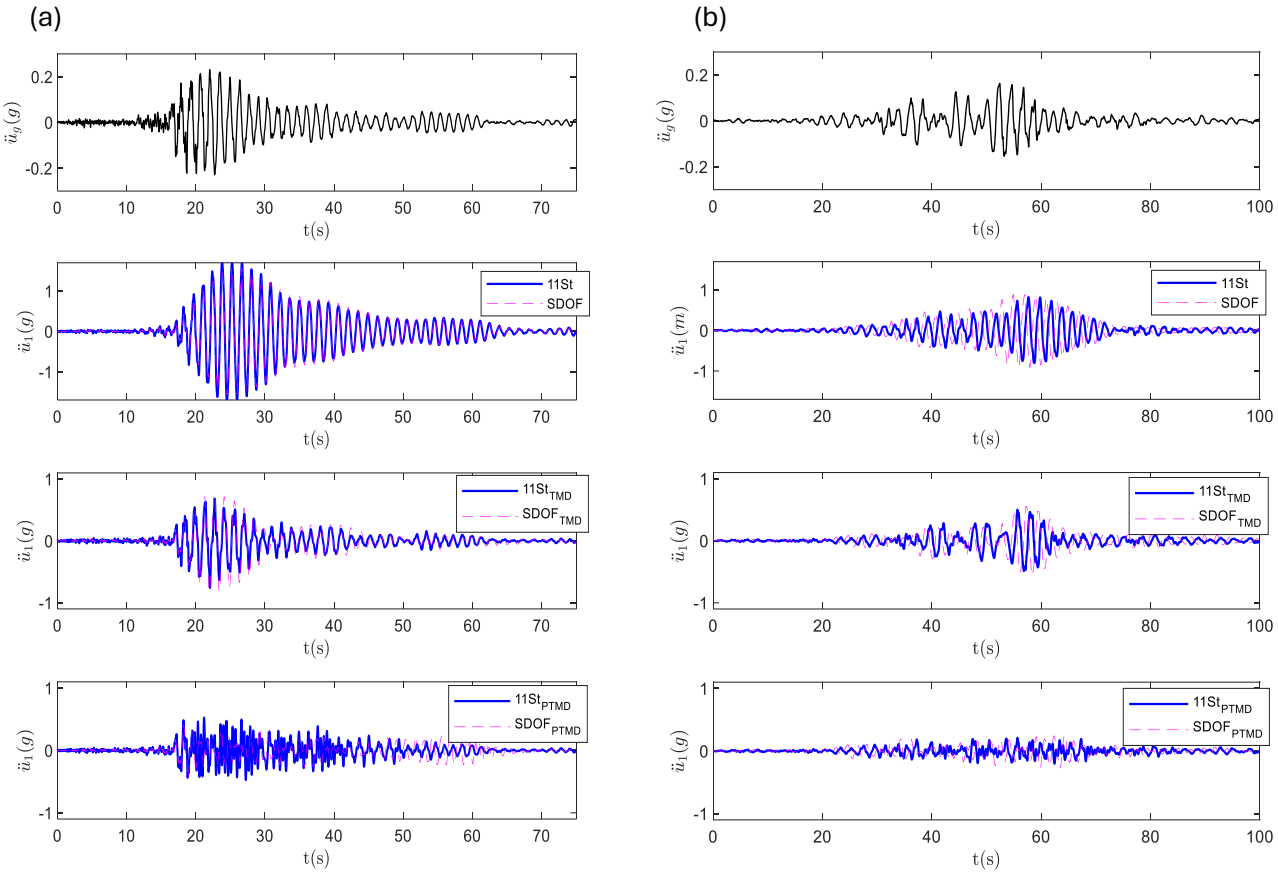

Fig 10. Acceleration history-time response of 11- and 17-storey systems at the top subjected to the September 19th 2017 (left) and September 19th 1985 (right) earthquakes, respectively, recorded at CH84 station with $PGA = 0.23g, T_1 = 1.4\ s, T_2 = 0.6T_1, T_3 = T_2, \gamma = 0.2, \beta = 1, d = 0.2m$; and SCT station with $PGA = 0.16g, T_1 = 2\ s, T_2 = 0.7T_1, T_3 = T_2, \gamma = 0.2, \beta = 1, d = 0.2m$. 1st row from top: input ground motion; 2nd row from top: frame without dampers; 3rd row: frame with TMD and 4th row: frame with PTMD. The solid and dashed lines in each plot are the response of MDOF and SDOF systems, respectively.

3.3.3 Peak response along the height of the buildings

Results for the structural response of the 11- and 17-storey buildings discussed above can be directly observed in Fig. 11, where the median peak response along the height of the buildings is shown for the synthetic ground motions described previously. Figure 11 shows an evident decrease in the median peak displacement when the buildings are provided with TMD (solid green lines) and PTMD (solid pink lines) systems versus the case without damper (solid blue lines). Therefore, using TMD or PTMD systems is a very effective measure to reduce peak responses along the height of the buildings when they are subjected to narrow-band ground-motions, especially for $T_1/T_s \sim 1$ and for the first mode of the frame being dominant. Additionally, it can be observed that smaller displacements are achieved with the use of PTMD systems for the synthetic ground motions. The standard errors, σ, are 0.40, 0.36 and 0.22 for 11-storey buildings without damper, TMD and PTMD, respectively. Similarly, σ values are 0.44, 0.38 and 0.24 for 17-storey buildings

without damper, TMD and PTMD, respectively. This means that buildings with PTMDs are more reliable than those with TMDs or without dampers.

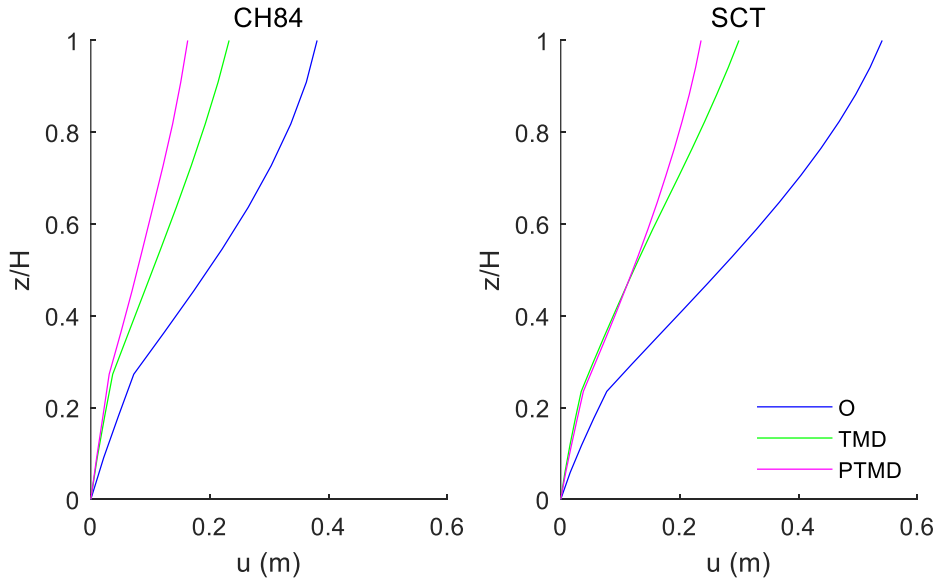

Fig 11. Median peak displacement response along the relative height (z/H) of the 11- and 17-storey buildings studied in the previous sections under the set of synthetic ground motions: blue, green, and pink lines correspond to the cases without damper, with TMD and with PTMD, respectively.

Conclusions

This study evaluates the effectiveness of Particle Tuned Mass Dampers (PTMD) in reducing maximum lateral displacements and accelerations in buildings subjected to narrow-band seismic excitations. Three configurations were analyzed: 1) a single-degree-of-freedom (SDOF) system without dampers; 2) a SDOF system with a Tuned Mass Damper (TMD); and 3) a SDOF system with a PTMD. Five key parameters seem to characterize the response of the SDOF system with a PTMD. (1) The period ratio between the PTMD container and SDOF oscillator, T_2/T_1; (2) the period ratio between the particle and the container, T_3/T_2; (3) the mass ratio between the container and SDOF oscillator, m_2/m_1; (4) the mass ratio between the particle and the container, m_3/m_2; and (5) the gap clearance between the particle and the container, d. When $T_2/T_1 < 1$ and d is small, the system with PTMD achieves smaller displacements than those with TMD or simply SDOF. When $T_3/T_2 > 1$, the SDOF maximum displacements tend to increase. When $m_2/m_1 > 0.1$ and d is small, smaller displacements can be achieved with respect to those with TMD or simply SDOF systems. When $m_3/m_2 > 1$ and d is small, smaller displacements can be achieved with respect to those with TMD or simply SDOF oscillators.

The results show that the dynamic responses of 11-storey and 17-storey elastic frames equipped with TMDs and PTMDs align well with those predicted by the governing equations of the corresponding SDOF models. Therefore, the simplified model used to characterize the PTMDs in buildings proves to be reliable and effective. This strongly supports the use of simplified SDOF-based analyses as a valid and practical tool for preliminary PTMD design in multi-degree-of-freedom structures. In particular, PTMDs can effectively

reduce the lateral response of the primary structural system when the frequency ratio between the predominant ground motion and the building approaches unity and the first mode dominates the response.

Furthermore, the results indicate a clear reduction in median peak displacements when PTMDs or TMDs are implemented, compared to the case without any damping device. PTMDs also tend to reduce floor accelerations under narrow-band seismic excitations, especially when the ground motion frequency and the building's natural frequency are close. Although PTMDs may sometimes offer slightly less reduction than conventional TMDs, they still present a viable and efficient alternative for passive control under narrow-band seismic conditions.

The findings of this study offer valuable guidance for practicing engineers in assessing the feasibility of implementing PTMDs in new or existing structures exposed to narrow-band earthquake excitations. The parametric insights, supported by comparisons with realistic building models, provide a practical and technically sound foundation for the design and deployment of PTMDs, especially in highly seismic areas like Mexico City, where the dominant frequency content of ground motions can coincide with the natural periods of buildings, making effective vibration mitigation not only beneficial but essential.

Acknowledgments

This research was financially supported by Instituto de Ingeniería at UNAM through the Research Fund R528. Additional support was sponsored by UNAM-PAPIIT under project number IG100623 “Evaluación del daño acumulado por efectos sísmicos y corrosivos durante el ciclo de vida en edificios de concreto reforzado”.

Appendix A. Contours of maximum displacements of the container

Additional figures are presented to illustrate the maximum displacements of the PTMD container u_2, as a function of four key system parameters that influence the vibration control performance of PTMDs. As shown in Figure A1, the displacement u_2 of the PTMD container can be comparable to—or even exceed—the displacement of the primary structure u_1 (see Figure 5), particularly when the system is not optimally tuned. For example, in panels (a) and (b), large values of u_2 (close to or above 1.0 m) occur when the period ratios $T_2/T_1 \approx 1$ or $T_3/T_2 > 1$, especially for large gap values d. This behavior is indicative of inefficient energy transfer and potential internal resonance within the PTMD.

Conversely, under favorable configurations—such as $T_2/T_1 < 1$, $m_2/m_1 > 0.1$, and small values of d—the displacement of the container u_2 remains moderate (typically $u_2 < 0.6$ m), while achieving significant reduction in the response of the main structure. These findings underscore the importance of carefully selecting the tuning parameters to limit excessive internal motion and ensure optimal energy dissipation through the PTMD system.

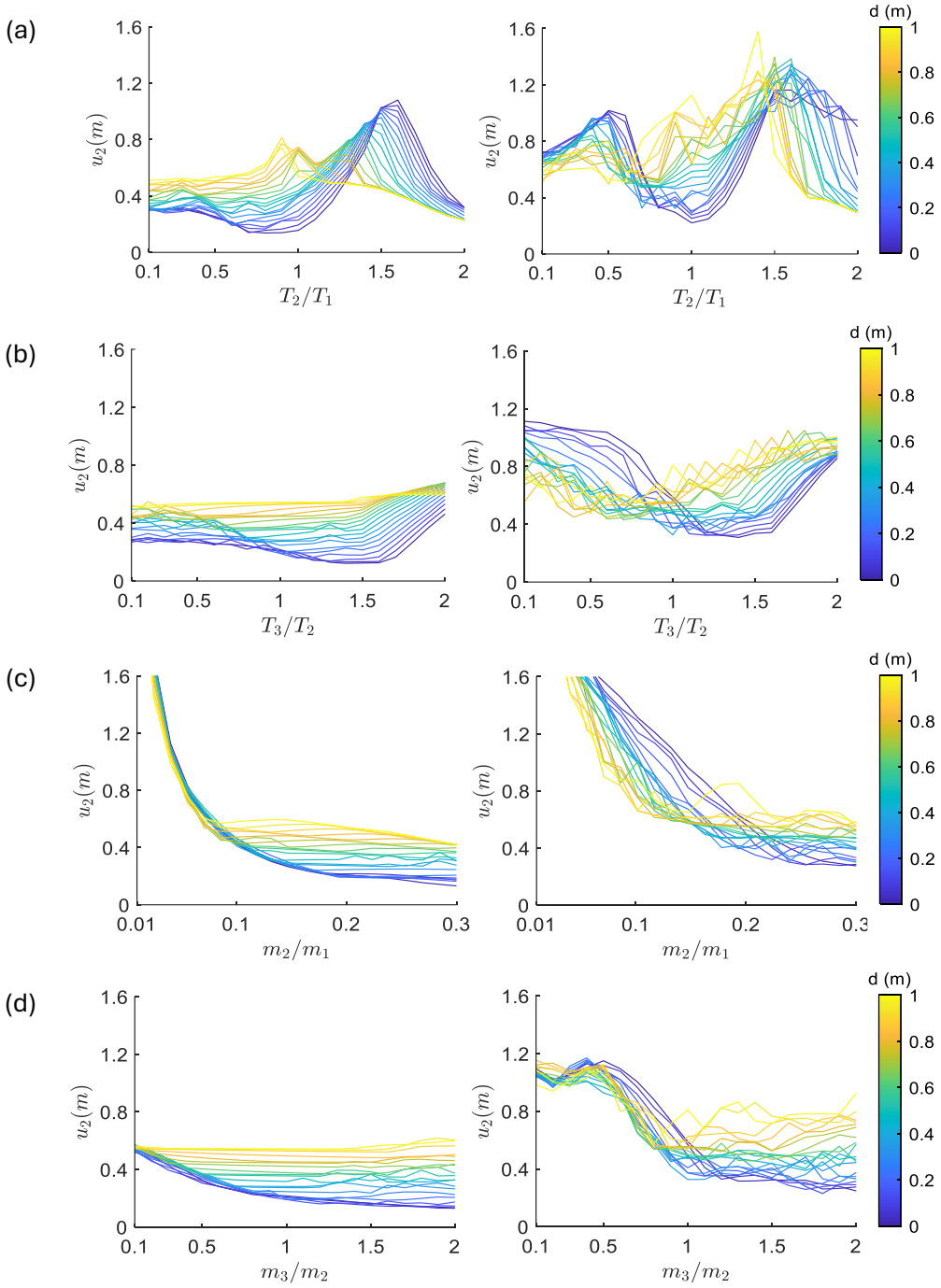

Fig A1. Contours of maximum displacements of the container u_2 (in meters) for SDOF systems with PTMD (solid line) subjected to the motions CH84-17 (left, $T_1 = 1\ s$) and SCT-85 (right, $T_1 = 2\ s$) considering the effects of: (a) the period ratio between the container and the SDOF oscillator T_2/T_1; (b) the period ratio between the particle and the container T_3/T_2; (c) the mass ratio between the container and SDOF oscillator m_2/m_1; and (d) the mass ratio between the particle and the container m_3/m_2. Properties similar to those of Figure 5 were considered.

References

[1] Rajkumari, S., Thakkar, K., and Goyal, H. Fragility analysis of structures subjected to seismic excitation: A state-of-the-art review, Structures, Volume 40, 2022, Pages 303-316.

[2] Frahm, H. Vibrations of bodies, Apr. 18, 1911. US Patent 989,958.

[3] Ormondroyd, J. Theory of the dynamic vibration absorber. Transaction of the ASME 50 (1928), 9–22.

[4] Den Hartog, J. Mechanical vibrations. McGraw-Hill, 1940.

[5] Vickery, B.J., Davenport, A.G. and Wargon, C. (1970), An Investigation of the Behaviour in wind of the proposed Centrepoint Tower In Sydney, Australia, boundary layer wind tunnel laboratory, Faculty of Engineering Sciences, University of Western Ontario, London, Ontario, Canada.

[6] Petersen, N.R. (1980). Design of large scale tuned mass dampers, Struct. Control, 581-596.

[7] Campbell, R. (1995). A true tall tale about the Hancock Tower, Boston Globe. 3.

[8] Ghorbani-Tanha, A.K., Noorzad, A. and Rahimian, M. (2009), "Mitigation of wind-induced motion of Milad Tower by tuned mass damper", Struct. Des. Tall Spec. Build., 18(4), 371-385.

[9] Lu, X. and Chen, J. (2011a). Mitigation of wind-induced response of Shanghai Center Tower by tuned mass damper, Struct. Des. Tall Spec. Build., 20(4), 435-452.

[10] Lu, X. and Chen, J. (2011b). Parameter optimization and structural design of tuned mass damper for shanghai centre tower, Struct. Des. Tall Spec. Build., 20(4), 453-471.

[11] Lu, Z., Wang, D., & Li, P. (2014). Comparison study of vibration control effects between suspended tuned mass damper and particle damper. Shock and Vibration, 2014.

[12] Roozbahan, M., and Turan, G (2023). An improved passive tuned mass damper assisted by dual stiffness, Structures, 50, 1598-1607.

[13] Fatollahpour, A., Tafakori, E., and Seyyed Ali Asghar Arjmandi (2023). The effects of structure-soil-structure interaction on seismic response of high-rise buildings equipped with optimized tuned mass damper, Structures, 50, 998-1010.

[14] Masri, S. F., & Ibrahim, A. M. (1973). Response of the impact damper to stationary random excitation. The Journal of the Acoustical Society of America, 53(1), 200-211.

[15] Bryce, L.F., Eric, M.F. and Steven, E.O. (2000). Effectiveness and predictability of particle damping, Proceedings of the SPIE's 7th Annual International Symposium on Smart Structures and Materials, International Society for Optics and Photonics.

[16] Hu, L., Huang, Q.B. and Liu, Z.X. (2008). A non-obstructive particle damping model of DEM, Int. J. Mech. Mater. Des., 4(1), 45-51.

[17] Sims, N.D., Amarasinghe, A. and Ridgway, K. (2005), "Particle dampers for workpiece chatter mitigation", Manuf. Eng., 16(1), 825-832.

[18] Li, K., & Darby, A. P. (2006). Experiments on the effect of an impact damper on a multiple-degree-of-freedom system. Journal of Vibration and Control, 12(5), 445-464.

[19] Papalou, A. and Masri, S.F. (1996), "Performance of particle dampers under random excitation", J. Vib. Acoust. T- Asme. 118(4), 614-621.

[20] Papalou, A. and Strepelias, E. (2014). "Effectiveness of particle dampers in reducing monuments' response under dynamic loads", Mech. Adv. Mater. Struct., 23 (2),128-135.

[21] Inoue, M., Yokomichi, I., & Hiraki, K. (2011). Particle damping with granular materials for multi degree of freedom system. Shock and vibration, 18(1-2), 245-256.

[22] Sánchez, M., & Carlevaro, C. M. (2013). Nonlinear dynamic analysis of an optimal particle damper. Journal of Sound and Vibration, 332(8), 2070-2080.

[23] Yan, W., Wang, B., & He, H. (2020). Research on damping mechanism and parameter analysis of particle damper based on energy theory. Journal of Engineering Mechanics, 146(6), 04020054.

[24] Jaimes, M., & Godínez, F. (2024). Efectividad de amortiguadores de partículas en edificios sujetos a excitaciones sísmicas de banda estrecha, Revista de Ingeniería Sísmica, 113, 115-133 (in Spanish).

[25] Simonian, S., & Brennan, S. (2005). Particle Tuned Mass Dampers: Design, Test, and Modeling. In 46th AIAA/ASME/ASCE/AHS/ASC Structures, Structural Dynamics and Materials Conference (p. 2325 9. 10.2514/6.2005-2325.

[26] Lu, Z., Wang, D., Masri, S. F., & Lu, X. (2016). An experimental study of vibration control of wind-excited high-rise buildings using particle tuned mass dampers. Smart Structures and Systems, 18(1), 93–115.

[27] Yan, W., Xu, W., Wang, J., Chen, Y. (2014). Experimental research on the effects of a tuned particle damper on a viaduct system under seis-mic loads. J. Bridge Eng. 19, 04013004.

[28] Li, S., Tang, J., (2017). On vibration suppression and energy dissipation using tuned mass particle damper. Journal of Vibration and Acous-tics, Transactions of the ASME 139, 1–10.

[29] Lu, Z, Wang, Z, Masri, SF, Lu, X. (2018a). Particle impact dampers: Past, present, and future. Struct Control Health Monit; 25:e2058.

[30] Liu, S, Lu, Z, Li, P, Zhang, W, Taciroglu, E. (2020). Effectiveness of particle tuned mass damper devices for pile-supported multi-story frames under seismic excitations. Struct Control Health Monit. 2020; 27:e2627.

[31] Lu, Z., Masri, S. F., & Lu, X. (2020). Particle Damping Technology Based Structural Control. Springe, ISBN 978-981-15-3498-0.

[32] Lu, Z., Zhang, J., Wang, D. (2021). Energy analysis of particle tuned mass damper systems with applications to MDOF structures under wind-induced excitation. Journal of Wind Engineering and Industrial Aerodynamics, 218, 104766, 1-17.

[33] Ogawa, K., T. Ide, and T. Saitou (1997). Application of impact mass damper to a cable-stayed bridge pylon. Journal of Wind Engineering and Industrial Aerodynamics 72 (1–3), 301–312.

[34] Naeim, F., et al. (2011). Performance of tall buildings in Santiago, Chile during the 27 February 2010 offshore Maule, Chile earthquake. The Structural Design of Tall and Special Buildings 20 (1), 1–16.

[35] Lu, Z., Chen, X., & Zhou, Y. (2018b). An equivalent method for optimization of particle tuned mass damper based on experimental parametric study. Journal of Sound and Vibration, 419, 571-584.

[36] Lu, Z., Chen, X., Zhang, D., & Dai, K. (2017). Experimental and analytical study on the performance of particle tuned mass dampers under seismic excitation. Earthquake Engineering & Structural Dynamics, 46(5), 697-714.

[37] Teran-Gilmore, A., & Jirsa, J. O. (2007). Energy demands for seismic design against low-cycle fatigue. Earthquake Engineering & Structural Dynamics, 36(3), 383-404.

[38] Den Hartog, J. P. (1947). The Undamped and Damped Dynamic Vibration Absorbers. Mechanical Vibrations, 3, 112-113.

[39] Jerome, J. C. (2002). Introduction to structural motion control. Prentice Hall Pearson Education, Inc., Upper Saddle River, New Jersey, 7458, 217-285.

[40] Butcher, J. C. (2016). Numerical methods for ordinary differential equations. John Wiley & Sons.

[41] SAP2000 (2016). Computers and Structures, Inc. SAP2000 Integrated Software for Structural Analysis and Design, Version 17.2.0. Berkeley, CA: Computers and Structures, Inc.

[42] NTCS-2023. Normas técnicas complementarias para diseño por sismo, Reglamento de Construcciones para el Distrito Federal, Gaceta Oficial del Departamento del Distrito Federal; 2023 (in Spanish).